Applied Catalysis B: Environmental 97 (2010) 198–203

Contents lists available at ScienceDirect

Applied Catalysis B: Environmental

journal homepage: www.elsevier.com/locate/apcatb

High photocatalytic activity of ZnO and ZnO:Al nanostructured films deposited by spray pyrolysis

Monserrat Bizarro*

Instituto de Investigaciones en Materiales, Universidad Nacional Autónoma de México, A. P. 70-360, Coyoacán C.P. 04510, D.F., Mexico

ARTICLE INFO

Article history:
Received 9 November 2009
Received in revised form 27 January 2010
Accepted 31 March 2010
Available online 8 April 2010

Keywords:
Zinc oxide
Photocatalysis
Spray pyrolysis

ABSTRACT

Zinc oxide and aluminum doped zinc oxide films were produced using the spray pyrolysis technique. The substrate temperature and the solution flow rate were varied to optimize the surface morphology of the films. Different concentrations of aluminum were added to the precursor solution in Al/Zn = 0.05, 0.10, 0.25, and 0.50 to study the effect on the photocatalytic activity of ZnO. The films were characterized by profilometry, scanning electron microscopy (SEM), X-ray diffraction (XRD) and the photocatalytic activity was tested by the decomposition of methyl orange dye under UV illumination. The addition of aluminum did not change the ZnO crystalline structure, but changed the surface morphology and increased the photocatalytic activity of ZnO films reducing the time taken to degrade an 80% of the dye from 4 to only 1.25 h.

1. Introduction

Heterogeneous photocatalysis process has been established as an efficient technique for the mineralization of toxic organic compounds, bacteria elimination, self-cleaning, etc. and thus, constitutes a potential process for environmental remediation. This is achieved by the strong oxidative ability of the photocatalyst, due to the ease of $OH^{\bullet}$ radical formation. Some semiconductor oxides present photocatalytic properties, being titanium dioxide (TiO_2) the widest studied and used for this purpose [1–3]. However, current investigations reveal that zinc oxide is also an efficient photocatalyst [4–8]. The reasons for the high photocatalytic efficiency of ZnO are attributed to the ability to generate H_2O_2 more efficiently than TiO_2 [9,10], as well as a higher number of active sites with high surface reactivity. Several reports refer to the synthesis and properties of ZnO nanoparticles, powders and colloids giving very high photocatalytic efficiencies and good stability [11,12]. But for water treatment applications, thin films are preferred to avoid the separation of the catalyst after the detoxification process. Diverse techniques have been used to produce ZnO films, such as evaporation [6], sputtering [13], sol–gel [14], pulsed laser deposition [15] and spray pyrolysis [16–18]. The spray pyrolysis is a simple and low cost technique, which can be scaled to large areas. Moreover, by manipulating its different deposition parameters, one can control the surface features of the films. It has been demonstrated that the spray pyrolysis technique is a good method to produce nanostructured metal oxides films like CeO_2 [19] yttria stabilized zirconia [20], tin oxide [21], among others. It was reported by Htay et al. [22] that by introducing a metal as a doping element in the spray solution, like Indium, a rod-shape crystal growth is favored, modifying drastically the surface. The work from Ullah and Dutta reports manganese doped ZnO nanoparticles to introduce tail states within the ZnO bandgap that increases the optical absorption at lower energies [12]. Aluminum doped zinc oxide has been studied as a transparent conducting oxide [23,24]; however, up to the author's knowledge, this material has not yet been studied as a photocatalyst.

In this work, structured ZnO and aluminum doped ZnO films with high photocatalytic activity were produced by the spray pyrolysis technique. The influence of different deposition parameters in the surface formation and the photocatalytic response of the doped and undoped samples were studied. In particular, it was found that the aluminum concentration plays a key role in the films growth and photocatalytic degradation of methyl orange dye. The advantages of using these materials as thin films are: (i) the elimination of filtration or separation steps after the dye removal, and (ii) the short time required for the complete degradation of the dye.

2. Experimental

The pneumatic version of the spray pyrolysis technique consists on the formation of droplets of a precursor solution by a high speed stream of air that mixes and passes through a nozzle. Friction between the liquid and air accelerates and disrupts the fluid stream and causes atomization. The formed droplets fall over a heated substrate where the chemical reactions take place forming the film.

* Tel.: +52 55 56224770x45671; fax: +52 55 56161251.
E-mail address: monserrat@iim.unam.mx.

0926-3373/$ – see front matter © 2010 Elsevier B.V. All rights reserved.
doi:10.1016/j.apcatb.2010.03.040

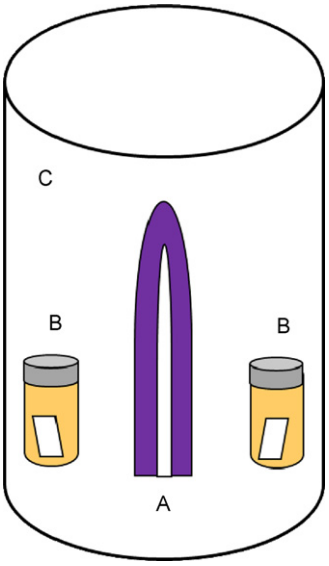

Fig. 1. Schematic representation of the photocatalytic reactor. (A) UV lamp of 7 W, (B) vials containing MO dye solution and the semiconductor films. The system affords up to 5 vials; (C) lamp casing.

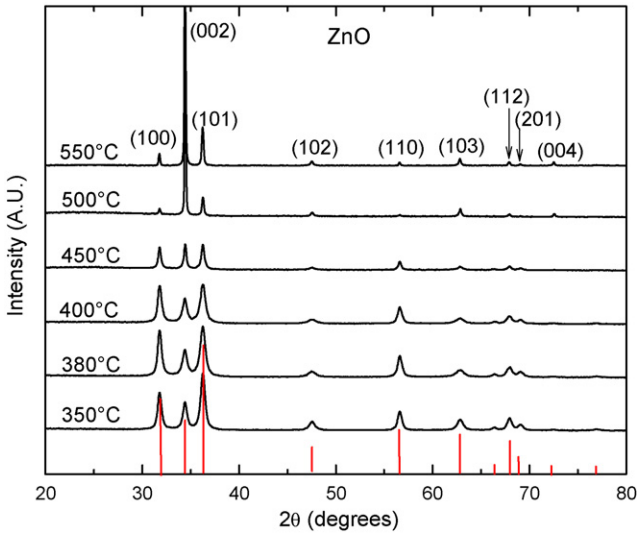

Fig. 2. XRD spectra of ZnO films growth at different substrate temperatures. The bottom red lines represent the reference positions of the powder diffraction peaks of hexagonal ZnO (pattern 01-089-1397). (For interpretation of the references to color in this figure legend, the reader is referred to the web version of the article.)

Zinc oxide films were obtained by the pneumatic spray pyrolysis technique using a 0.2 M solution of zinc acetate ($Zn(CH_3COO)_2{\cdot}2H_2O$, 98% purity from Sigma–Aldrich) dissolved in deionized water ($\rho \geq 15\,M\Omega\,cm$). The films were formed at different substrate temperatures, from 350 to 550 °C, in order to study the grain growth and a possible phase transformation. These films were deposited using a constant gas flow rate (F_g) of 8 L/min and a solution flow rate (F_s) of 18.2 mL/min. Then, the second parameter to be varied was the solution flow rate from 8.0 to 21.8 mL/min, keeping the gas flow rate at a constant value of 8 L/min and a substrate temperature of 400 °C. The nozzle was kept at a constant distance from the substrate (32 cm) in all cases. The films were deposited onto pyrex glass substrates of 1×0.5 inches ultrasonically cleaned with trichloroethylene (99.5% from Sigma–Aldrich), acetone (99.6%, from J.T. Baker) and methanol (99.93% from Sigma–Aldrich). All the solvents and reactants were used as purchased.

The third parameter that was analyzed was the doping concentration. Aluminum doped zinc oxide (ZnO:Al) films were obtained by adding aluminum chloride ($AlCl_3{\cdot}6H_2O$, 99% purity from Aldrich) to the previous zinc acetate solution in the following Al/Zn ratios: 0.05, 0.10, 0.25 and 0.50. These samples were deposited at 500 °C and the gas and solution flow rates were fixed at 8 L/min and 14.6 mL/min respectively.

X-ray diffraction (D8 Advance Bruker) was used to determine the crystalline structure of the films, using the Cu $K\alpha_1$ wavelength (1.54056 Å). The morphology of the films was studied by scanning electron microscopy (SEM) (Leyca Cambridge 400). The thickness and roughness of the films were measured with a profilometer (Sloan DekTac IIA).

The photocatalytic activity of the films was studied by the degradation of an aqueous solution of methyl orange dye ($C_{14}H_{14}N_3SO_3Na$, 85% from Sigma–Aldrich) in a concentration of 10^{-5} M. The samples were immersed in 10 mL of the dye solution with a pH of 6.8 and were irradiated with a 7 W UV lamp with main emission at 380 nm (measured with a spectrofluorometer SPEX Fluoromax) and a luminance of 5.2 ± 0.1 cd/m^2 (Minolta camera LS-110). The experimental set-up for the photocatalytic reactor is shown in Fig. 1.

The change in optical absorption of the dye was measured as a function of the irradiation time with a UV spectrophotometer (JASCO V620) from 190 to 800 nm, using deionized water in the reference beam. The degradation percentage was obtained as well as the rate of reaction k. This rate of reaction was used to compare the efficiency of the catalysts.

3. Results

The deposition temperature is an important parameter during the film's growth by spray pyrolysis. This temperature was varied from 350 to 550 °C to form ZnO films. These samples were studied by X-ray diffraction, to obtain the crystalline structure and the grain size. As it can be seen in Fig. 2, all the films presented the same hexagonal phase. But at high temperatures the films present preferential growth, that can be appreciated in the excessive growth of (0 0 2) peak. The grain size of these samples was estimated using the Scherrer's formula written below, applied to the (0 0 2) peak:

$$d = \frac{0.9\lambda}{B\cos\,\theta} \quad (1)$$

where d is the grain size, λ is the wavelength of X-ray, B is the broadening of the full width at half maximum and θ the Bragg's angle. These values are listed in Table 1. The grain size increased from 30 nm of the film deposited at 350 °C to 97 nm of the sample grown at 550 °C, as it is expected for the normal crystal growth. It was observed that for a temperature of 450 °C the film has the greatest thickness and also rougheness (which is desired for photocatalysis), and at 550 °C the thickness decreases and the film looses adhesion to the substrate. This is due to the evaporation of the solvent before the droplets arrive to the substrate giving place to the formation of powder particles that can be easily removed from the

Table 1
Structural characteristics of ZnO films at different temperatures.

Substrate temperature (°C)	Grain size (nm)	Thickness (μm)	Roughness (μm)
350	30	17.39	0.51
380	26	15.60	2.62
400	27	23.14	2.33
450	52	8.05	7.15
500	90	1.31	0.59
550	97	1.27	0.04

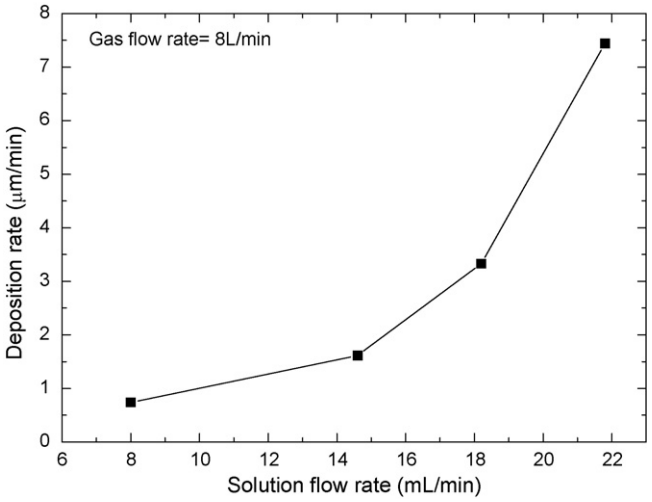

Fig. 3. Deposition rate of the films as a function of the solution flow rate.

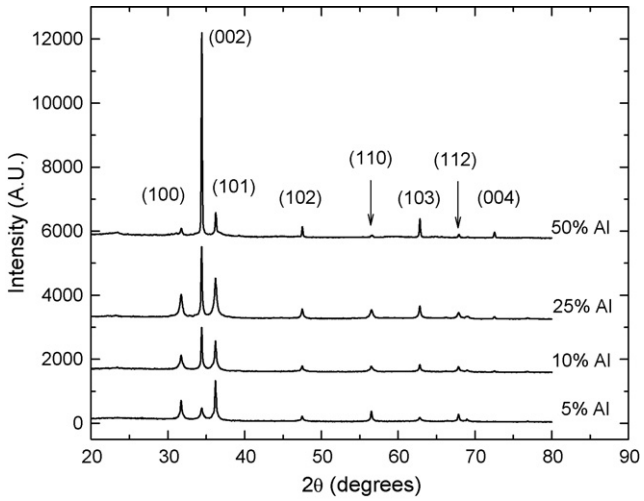

Fig. 4. XRD of ZnO:Al films with different aluminum concentrations deposited at 500 °C, F_g = 8 L/min and F_s = 14.6 mL/min.

substrate. At 500 °C the films are rough but they are still adhered to the substrate, for this reason it was selected as the temperature for further depositions.

The second studied parameter was the solution flow rate. This parameter is related to the amount of mass that arrives to the substrate, which will control the deposition rate. The solution flow rate was varied from 8.0 to 21.8 mL/min for a constant gas flow rate of 8 L/min. The relation between the deposition rate and the solution flow rate is shown in Fig. 3, which presents an increasing behavior as the solution flow rate is higher. The quick increase of the deposition rate originates less homogeneous films with higher roughness. For photocatalytic applications a rough surface is beneficial because it gives more contact area [25]; however the film's quality can be diminished by the low adhesion. For this reason, for the next deposits an intermediate solution flow rate was

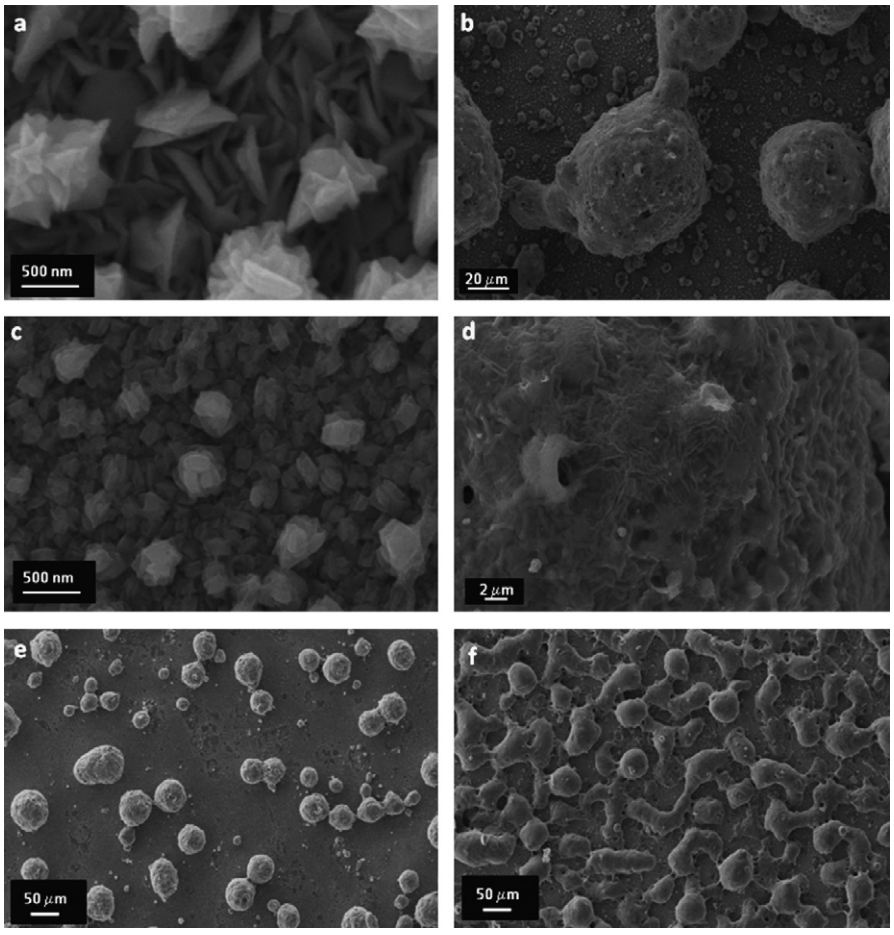

Fig. 5. SEM images of ZnO (a) and ZnO:Al-5% films (b); zoom of the bottom layer of ZnO:Al-5% (c); zoom of one ball of ZnO:Al-5% constituted by thin fibers (d); ZnO:Al-25% film (e) and ZnO:Al-50% film (f).

Table 2
Characteristics of the films with different aluminum concentrations and their rates of reaction.

Sample name	Grain size (nm)	Thickness (μm)	Roughness (μm)	Thickness/mass ratio ($\times 10^{-3}$ m/g)	k (h^{-1})
ZnO	90	1.31	0.59	0.34	0.367
ZnO:Al-5%	55	3.39	2.48	0.33	0.381
ZnO:Al-10%	99	16.09	14.51	0.92	0.872
ZnO:Al-25%	90	24.93	12.40	0.95	1.232
ZnO:Al-50%	124	29.14	9.32	0.81	1.359

Sample name	Al/Zn in solution	Al/Zn incorporated	Cl/Zn incorporated
ZnO	0	0	0
ZnO:Al-5%	0.05	0.06	0.01
ZnO:Al-10%	0.10	0.08	0.02
ZnO:Al-25%	0.25	0.12	0.05
ZnO:Al-50%	0.50	0.32	0.23

selected, that provide rough films but with good adhesion to the substrate.

Considering the previous results, aluminum doped zinc oxide films were prepared at selected conditions (T = 500 °C, F_g = 8 L/min, F_s = 14.6 mL/min). XRD patterns were obtained to study the crystalline structure and grain size. The hexagonal phase of ZnO was not modified by adding aluminum up to an Al/Zn ratio of 0.50 in solution. But the preferential growth along the (0 0 2) peak increased with the aluminum content, as it can be seen in Fig. 4.

The surface morphology also changes when aluminum is incorporated to the films. Fig. 5 shows a comparison of the surface morphology, observed by SEM, of samples with and without aluminum. In the case of ZnO films, the surface of the film is composed by thin triangular plates with an approximate length of 500 nm that give a large surface area (Fig. 5(a)). When aluminum is incorporated to the films, the surfaces present a very different morphology (Figs. 5(b)–(f)). The bottom layer is constituted by crystalline shapes that are similar to those in the undoped sample (Fig. 5(c)); but on the upper part, big rounded features of ~50 μm diameter appear. These balls present a fiber structure that can be appreciated in Fig. 5(d). As the aluminum content increases, the number of balls also increases. The presence of these big-sized-balls largely improves the photocatalytic properties in comparison with a flat surface. Energy dispersive X-ray spectroscopy (EDS) was used to obtain the composition of the films, in order to determine the proportion of aluminum that was effectively incorporated to the films; these values of the Al/Zn ratio are presented in Table 2, and show that a smaller fraction of aluminum was incorporated to the films, specially for the one with the highest Al content in the precursor solution. Moreover, EDS technique also indicated the presence of chlorine in the films, due to the Al precursor, that increases as the aluminum content is augmented.

Photocatalytic tests were carried out for all the obtained films. The degradation of the methyl orange dye was measured by the diminution of its absorption band as a function of the UV irradiation time. An example of the absorption spectra evolution as a function of the illumination time is shown in Fig. 6 for the sample with Al/Zn = 0.5. Besides, Fig. 7 presents the degradation percentage calculated as follows, where A_0 and A are the absorbance maxima of the methyl orange dye before and after an irradiation time, respectively:

$$\text{degradation}\,\% = \left(1 - \frac{A}{A_0}\right) \times 100 \quad (2)$$

The pure ZnO film degraded an 80% of the dye solution in 4 h (not shown) and reached the 100% degradation until 8 h. In contrast, the film with Al/Zn = 0.50 degraded an 80% of the dye in only 1.25 h, three times faster than the pure ZnO film. It is also appreciated in Fig. 7, that the films with 0.25 and 0.50 Al/Zn ratios in solution had a similar response indicating a saturation tendency.

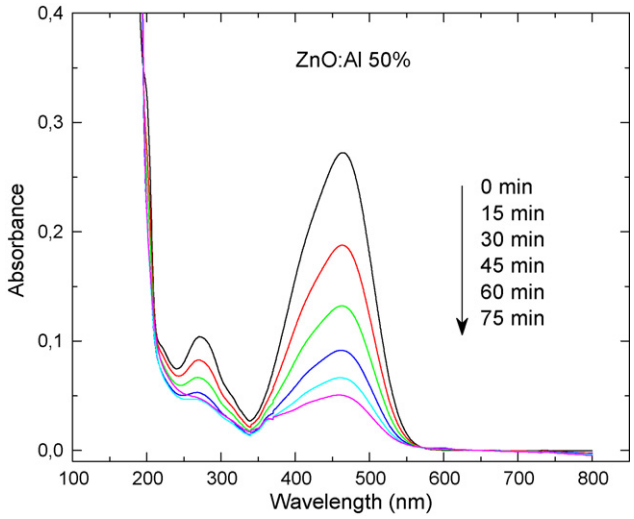

Fig. 6. Evolution of the absorption spectrum of MO with the illumination time.

To obtain the kinetics of the reaction, the $\ln(A_0/A)$ versus the irradiation time was plotted, giving straight lines that indicate first order reactions, shown in Fig. 8. The slopes of these lines correspond to the rate of reaction, shown in Table 2. It is clear in Fig. 8 that the increment in aluminum concentration gives a better photocatalytic response, but this improvement of activity is not proportional, it has a great improvement for 0.10 and 0.25 Al/Zn ratios, but for higher

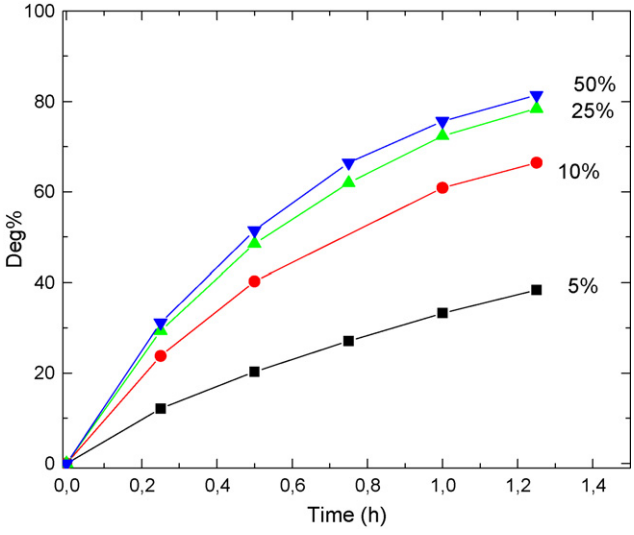

Fig. 7. Degradation percentage of samples with different aluminum concentration.

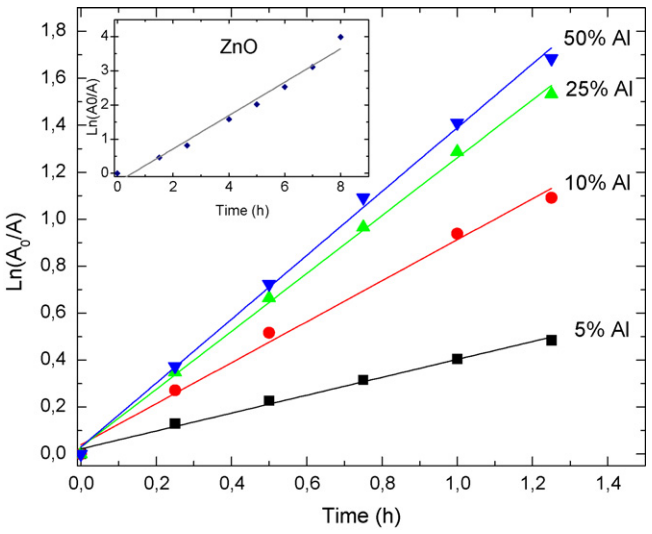

Fig. 8. Kinetics of reaction of MO dye given by ZnO films with different aluminum concentrations. The inset shows the kinetics of reaction obtained using the pure ZnO film.

concentrations this improvement reaches a saturation value, as it can be seen in Fig. 9.

4. Discussion

The photocatalytic degradation of the MO dye was greatly improved by doping the ZnO films with aluminum. Many factors can contribute to this enhanced activity. Firstly, as it was mentioned before, the addition of aluminum to the zinc precursor solution modifies notably the film growth, giving a different surface morphology and roughness, in one case triangular plates were formed, while in the other big balls appeared on the surface. This balls presented thin fibers in their surface, contributing to increase the active area. The formation of completely different surfaces of the films with and without aluminum may be due to the precursor of the dopant ($AlCl_3{\cdot}6H_2O$), the high substrate temperature and the high solution flow rate. All these factors may contribute to the formation of big drops of the Zn–Al solution that arrive to the substrate and do not react immediately, keeping a rounded shape. This fact suggests that a small part of the aluminum atoms do not penetrate into the ZnO matrix, forming perhaps an amorphous Al_2O_3 (not detectable by XRD); this could explain the diminution of the Al content in the films and the saturation tendency observed in the rate of reaction as a function of the aluminum concentration in solution. In addition, EDS analysis showed that the aluminum is present in a slightly higher proportion in the balls, whereas in the bottom layer the composition is mostly zinc oxide with a smaller fraction of aluminum (for instance, in sample with Al/Zn = 0.05 in solution it was found that $Al/Zn_{ball} \sim 0.1$, while the average value was $Al/Zn_{global} = 0.06$). Current investigations are been developed in order to understand the formation and morphology of the films.

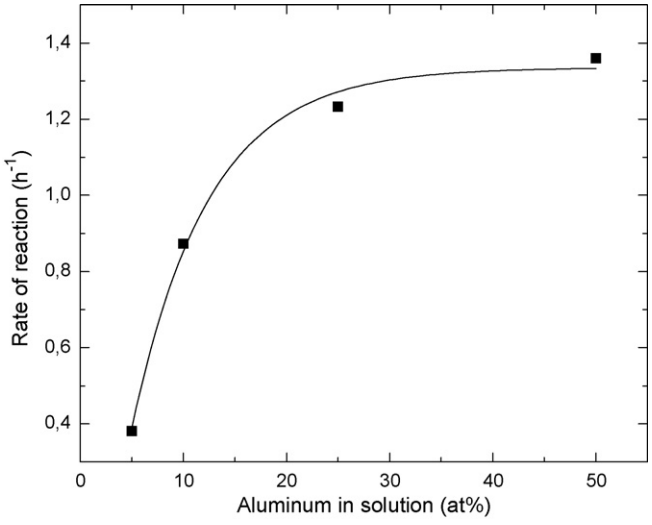

Fig. 9. Tendency of the rate of reaction obtained for the films with different aluminum concentrations.

In second place, it has to be mentioned that the photocatalytic activity depends on the surface and the quantity of catalyst loaded. For this reason, a thickness to mass ratio (T/m) was obtained for the films, shown in Table 2. This T/m ratio was about 0.3 for the samples with the lowest Al content and increased around 0.9 for the samples with the highest Al content. It is possible that the rate of reaction was affected by this trend; however the rate of reaction achieved for the sample with Al/Zn = 0.5 cannot be equaled by pure ZnO thicker films. So the aluminum dopant is an important factor in the reaction enhancement anyway.

Another factor that contributed to the improvement of the photocatalytic activity can be explained from a chemical point of view. The aluminum ions Al^{3+} that incorporate in the ZnO matrix substitute zinc ions Zn^{2+} providing an extra positive charge that remains available when the photochemical reactions start; however, a charge compensation may occur making the electrons of oxygen atoms redistribute towards those positive charges, and then a negative charge is now available. As it is known, ZnO:Al is considered an n-type semiconductor. This was confirmed by measurements using the hot probe technique to identify the type of the charge carriers [26]. When the semiconductor is illuminated, the generation of electrons and holes begins (Eq. (3)) and, as the semiconductor is immersed in a liquid medium, spontaneous adsorption of the molecules in the liquid occurs; then an electron is transferred to the acceptor molecule and the donor molecule gives an electron to the semiconductor film. The holes generate $OH^{\bullet}$ by reacting with the water molecules (Eq. (4)), and the O_2 molecule accepts an electron to form the super-oxide radical $O_2^{\bullet -}$ (Eq. (5)). These $O_2^{\bullet -}$ radicals act as very oxidizing agents and they are also contribute to the formation of hydrogen peroxide (Eqs. (6)–(9)) [25]. The formed radicals react with the dye molecule, disrupting it in its conjugated system which leads to the complete decomposition of the dye [3,11]. The presence of extra electrons contributes to the formation of $O_2^{\bullet -}$ radicals that accelerate the decomposition mechanism, reducing the dye discoloration time.

$$ZnO + h\nu \rightarrow e^- + h^+ \quad (3)$$

$$H_2O + h^+ \rightarrow OH^{\bullet} + H^+ \quad (4)$$

$$O_2 + e^- \rightarrow O_2^{\bullet -} \quad (5)$$

$$O_2^{\bullet -} + H^+ \rightarrow HO_2^{\bullet} \quad (6)$$

$$2HO_2^{\bullet} \rightarrow H_2O_2 + O_2 \quad (7)$$

$$H_2O_2 + O_2^{\bullet -} \rightarrow OH^{\bullet} + O_2 + OH^- \quad (8)$$

$$OH^{\bullet} + \text{dye} \rightarrow \text{dye mineralization} \quad (9)$$

The photocatalytic performance of ZnO and ZnO:Al films is greater than that obtained for TiO_2 films in our previous work, where the surface was modified to enhance the activity [25]. In that work, the TiO_2 films with TiO_2 P-25 nanopowder on the surface, degraded the MO dye in 6 h and gave a rate of reaction

of 0.416 h^{-1}. Comparing the TiO_2 films with ZnO:Al films, it is observed that even for the sample with Al/Zn = 0.10 the efficiency is double and for that with 0.25 the efficiency is three times greater than the obtained for TiO_2. Other authors like Ghorai et al. have reported the efficiency of TiO_2 and Fe(III) doped TiO_2 nanopowders in the degradation of organic dyes. They obtained rates of reaction of the order of 0.65 h^{-1} for $Fe_{0.005}Ti_{1-0.005}O_2$ powder and 0.576 h^{-1} for P25 [27]. The results here obtained for ZnO:Al films represent a promising photocatalytic material for water treatment applications.

5. Conclusions

The spray pyrolysis technique allowed the synthesis of pure and aluminum doped ZnO films with photocatalytic activity. Some of the deposition parameters were optimized to obtain films with adequate surface morphology, such as temperature and solution flow rate. The aluminum incorporated improved greatly the photocatalytic efficiency of ZnO films, reducing the degradation time of the MO dye from 4 to only 1.25 h (up to an 80% of degradation) following the next order of aluminum/zinc ratios added to the precursor solution: 0 < 0.05 < 0.10 < 0.25 < 0.50. The photocatalytic activity improvement increased greatly for 0.10 and 0.25 Al/Zn ratios, but for higher concentrations this improvement reached a saturation value. The good performance of aluminum doped ZnO films shows that it can be used as an effective photocatalyst for water treatment applications.

Acknowledgements

The author wishes to thank O. Novelo, A. Tejeda and L. Baños for technical support; Dr. A. Ortiz, Dr. J.C. Alonso and Dr. G. Santana for the facility to use the laboratories and equipments and Dr. M. Monroy, Dr. M. García and Dr. E. Ramos for the revision and comments to the manuscript. This work was supported by DGAPA under project IN-116109.

References

[1] K. Hashimoto, H. Irie, A. Fujishima, Jpn. J. Appl. Phys. 44 (12) (2005) 8269–8285.
[2] M.R. Hoffmann, S.T. Martin, W. Choi, D.W. Bahnemann, Chem. Rev. 95 (1995) 69–96.
[3] J.-M. Herrmann, Top. Catal. 34 (2005) 49–65.
[4] B. Pal, M. Sharon, Mater. Chem. Phys. 76 (2002) 82–87.
[5] S.K. Kansal, M. Singh, D. Sud, J. Hazard. Mater. 141 (2007) 581–590.
[6] A.A. Aal, S.A. Mahmoud, A.K. Aboul-Gheit, Mater. Sci. Eng. C 29 (2000) 831–835.
[7] E. Yassitepe, H.C. Yatmaz, C. Öztürk, K. Öztürk, C. Duran, J. Photochem. Photobiol. A 198 (2008) 1–6.
[8] H.-F. Lin, S.-C. Liao, S.-W. Hung, J. Photochem. Photobiol. A 174 (2005) 82–87.
[9] E.R. Carraway, A.J. Hoffman, M.R. Hoffman, Environ. Sci. Technol. 28 (1994) 786–793.
[10] A.J. Hoffman, E.R. Carraway, M.R. Hoffman, Environ. Sci. Technol. 28 (1994) 776–785.
[11] C.A.K. Gouvea, F. Wypych, S.G. Moraes, N. Durán, N. Nagata, P. Peralta-Zamora, Chemosphere 40 (2000) 433–440.
[12] R. Ullah, J. Dutta, J. Hazard. Mater. 156 (2008) 194–200.
[13] V. Tvarozek, I. Novotny, P. Sutta, S. Flickyngerova, K. Schtereva, E. Vavrinsky, Thin Solid Films 515 (2007) 8756–8760.
[14] D. Bao, H. Gu, A. Kuang, Thin Solid Films 312 (1998) 37–39.
[15] H. Kim, C.M. Glimore, J.S. Horwitz, A. Piqué, H. Murata, G.P. Kushto, R. Schalf, z.H. Kafafi, D.B. Chrisey, Appl. Phys. Lett. 76 (2000) 259.
[16] A. Sánchez-Juárez, A. Tiburcio-Silver, A. Ortiz, Solar Energy Mater. Solar Cells 52 (1998) 301–311.
[17] A. Ashour, M.A. Kaid, N.Z. El-Sayed, A.A. Ibrahim, Appl. Surf. Sci. 252 (2006) 7844–7848.
[18] M. Miki-Yoshida, V. Collins-Martínez, P. Amézaga-Madrid, A. Aguilar-Elguézabal, Thin Solid Films 419 (2002) 60–64.
[19] M.F. García-Sánchez, A. Ortiz, G. Santanta, M. Bizarro, J. Peña, F. Cruz-Gandarilla, M.A. Aguilar-Frutis, J.C. Alonso, J. Am. Ceram. Soc. (2009) (published online October 2009).
[20] M.F. García-Sánchez, J. Peña, A. Ortiz, G. Santana, J. Fandiño, M. Bizarro, F. Cruz-Gandarilla, J.C. Alonso, Solid State Ionics 170 (2008) 243–249.
[21] J.K. Yu, D.H. Kim, J. Ceram. Soc. Jpn. 117 (1370) (2009) 1078–1084.
[22] M.T. Htay, Y. Hashimoto, K. Ito, Jpn. J. Appl. Phys. 46 (2007) 440–448.
[23] C. Olivieira, L. Rebouta, T. de Lacerda-Aroso, S. Lanceros-Mendez, T. Siseu, C.J. Tavares, J. Tovar, S. Fredov, E. Alves, Thin Solid Films 517 (23) (2009) 6290–6293.
[24] Z. Ben Ayadi, L. El Mir, K. Djessas, S. Alaya, Thin Solid Films 517 (23) (2009) 6305–6309.
[25] M. Bizarro, M.A. Tapia-Rodríguez, M.L. Ojeda, A. Ortiz, Appl. Surf. Sci. 255 (2009) 6274–6278.
[26] W.R. Runyan, Semiconductor Measurements and Instrumentation, Texas Instruments Electronics Series, McGraw-Hill Book Co., Dallas, 1975.
[27] T.K. Ghorai, S.K. Biswas, P. Pramanik, Appl. Surf. Sci. 254 (2008) 7498–7504.